

A plant NLR receptor employs ABA central regulator PP2C-SnRK2 to activate antiviral immunity

Received: 26 July 2023

Accepted: 28 March 2024

Published online: 13 April 2024

 Check for updatesShen Huang¹, Chunli Wang¹, Zixuan Ding¹, Yaqian Zhao¹, Jing Dai¹, Jia Li¹, Haining Huang¹, Tongkai Wang¹, Min Zhu¹, Mingfeng Feng¹, Yinghua Ji², Zhongkai Zhang³ & Xiaorong Tao¹✉

Defence against pathogens relies on intracellular nucleotide-binding, leucine-rich repeat immune receptors (NLRs) in plants. Hormone signaling including abscisic acid (ABA) pathways are activated by NLRs and play pivotal roles in defence against different pathogens. However, little is known about how hormone signaling pathways are activated by plant immune receptors. Here, we report that a plant NLR Sw-5b mimics the behavior of the ABA receptor and directly employs the ABA central regulator PP2C-SnRK2 complex to activate an ABA-dependent defence against viral pathogens. PP2C4 interacts with and constitutively inhibits SnRK2.3/2.4. Behaving in a similar manner as the ABA receptor, pathogen effector ligand recognition triggers the conformational change of Sw-5b NLR that enables binding to PP2C4 via the NB domain. This receptor-PP2C4 binding interferes with the interaction between PP2C4 and SnRK2.3/2.4, thereby releasing SnRK2.3/2.4 from PP2C4 inhibition to activate an ABA-specific antiviral immunity. These findings provide important insights into the activation of hormone signaling pathways by plant immune receptors.

Defense against microbial pathogens relies on two tiers of innate immune system mediated by cell-surface pattern recognition receptors (PRRs) and intracellular nucleotide-binding domain-containing, leucine-rich repeat receptors (NLRs) in plants^{1–3}. PRRs recognize microbe-associated molecular patterns and initiate pattern-triggered immunity (PTI)^{4,5}, whereas NLRs detect pathogen effectors that interfere with host PTI and activate a robust disease resistance known as effector-triggered immunity (ETI)^{1–3}. The downstream immune outputs, including bursts of intracellular calcium, production of reactive oxygen species, and expression of defense genes, largely overlap in PTI and ETI^{6,7}. Compared to PTI, which confers a transient, mild, and basal defense, the defense of ETI is often faster, stronger, and more prolonged⁸. Recent studies have shown that PTI can amplify and boost the defense signaling of ETI^{9–12}. Despite this, the mechanism underlying how NLRs induce fast, strong, and prolonged defense in ETI remains largely unknown.

Hormone signaling pathways, including salicylic acid, jasmonic acid (JA), and ethylene signaling, are activated frequently by plant immune receptors^{13,14}. These hormone signaling pathways play important roles in plant defense against different pathogens. Abscisic acid (ABA) is a major stress phytohormone that responds to both abiotic stress and biotic stress^{15,16}. ABA was found to play a pivotal role in plant defenses against viruses, including *Bamboo mosaic virus* (BaMV), *Tobacco necrosis virus* (TNV), and *Chinese wheat mosaic virus* (CWMV)^{17–19}. The ABA-insensitive mutant *abi1-1* displayed greater susceptibility to BaMV¹⁷. Activation of the ABA signaling pathway was also found in Soybean NLR immune receptor *Rsv3*, which confers extreme resistance to *Soybean mosaic virus* (SMV); this activation of ABA signaling is important for callose deposition to plasmodesmata and inhibition of viral cell-to-cell movement²⁰. Despite these hormone signaling pathways are known to play pivotal roles in plant defense,

¹The Key Laboratory of Plant Immunity, Department of Plant Pathology, Nanjing Agricultural University, Nanjing 210095, P. R. China. ²Institute of Plant Protection, Jiangsu Academy of Agricultural Sciences, Nanjing 210014, China. ³Yunnan Academy of Tobacco Agricultural Sciences, Key Laboratory of Tobacco Biotechnological Breeding, National Tobacco Genetic Engineering Research Center, Kunming 650021, China. ✉e-mail: taoxiaorong@njau.edu.cn

little is known about how plant immune receptors, upon recognition of pathogens, initiate different hormone signaling pathways.

The major players of ABA signaling regulation include ABA receptors, protein phosphatases type-2C (PP2Cs), and sucrose-non-fermenting 1 (SNF1)-related kinases subfamily 2 (SnRK2s)^{21,22}. The pyrabactin resistance (PYR)/pyrabactin resistance-like (PYL)/regulation components of ABA receptors (RCARs) are ABA receptor that belong to the START superfamily²³. In the presence of ABA, the PYR/PYL/RCAR receptor complex undergoes conformational changes that enable binding to PP2C protein^{24–26}. PP2C-type protein phosphatases are monomeric enzymes with large members in plants, and Group A PP2Cs function as negative regulators in ABA signaling^{27,28}. SnRK2s phosphorylate and activate downstream factors²⁹. However, group A PP2Cs interact with and constitutively inactivate SnRK2^{29,30}. Thus, activation of SnRK2s is a key step in ABA signal transduction³¹. Upon the binding of ABA, PYR/PYL/RCAR receptors bind to PP2C^{24–26}, which competes with the interaction of SnRK2s with PP2C, thereby releasing SnRK2s from PP2C inhibition to activate downstream substrates and initiate ABA signaling²².

Tomato spotted wilt orthotospovirus (TSWV), one of the most destructive plant viruses, has resulted in an annual loss of over \$1 billion worldwide, posing a major threat to global crop productivity^{32,33}. The most effective measure for controlling TSWV is to use of resistant cultivars. The *Sw-5b* is the most widely used, effective resistance gene in tomato-resistant cultivar breeding to control TSWV³⁴. *Sw-5b* encodes an NLR immune receptor containing an N-terminal solanaceous-specific domain (SD), a coil-coil domain, an NB-ARC domain [nucleotide-binding (NB) adapters share sequence homology with Apaf-1, certain resistance proteins, and CED-4], and a leucine-rich repeat (LRR) domain^{35,36}. *Sw-5b* induces a strong disease resistance against TSWV upon the recognition of viral effector NSm³⁷, a movement protein that facilitates viral intercellular movement through dilating the size limit of plasmodesmata in the plant cell wall³⁸. Both SD and LRR domains are required for NSm recognition³⁹, whereas the NB domain of *Sw-5b* itself can trigger cell death, independent of the viral effector NSm⁴⁰.

In this study, we report that pathogen effector recognition by *Sw-5b* NLR induces an ABA-dependent antiviral immunity. Mechanically, we show that the *Sw-5b* NLR receptor mimics the behavior of the ABA receptors and employs the ABA central regulator PP2C4-SnRK2 complex to activate ABA signaling. Upon recognition of viral effector NSm, *Sw-5b* NLR undergoes conformational changes that allow it to bind to PP2C4 via the NB domain. The NBPP2C4 binding disrupts the interaction between PP2C4 and SnRK2.3/2.4, thereby releasing SnRK2 from PP2C inhibition for ABA-dependent defense against viral pathogens.

Results

The NB domain of *Sw-5b* interacts directly with group A PP2C4 and activates the ABA signaling pathway

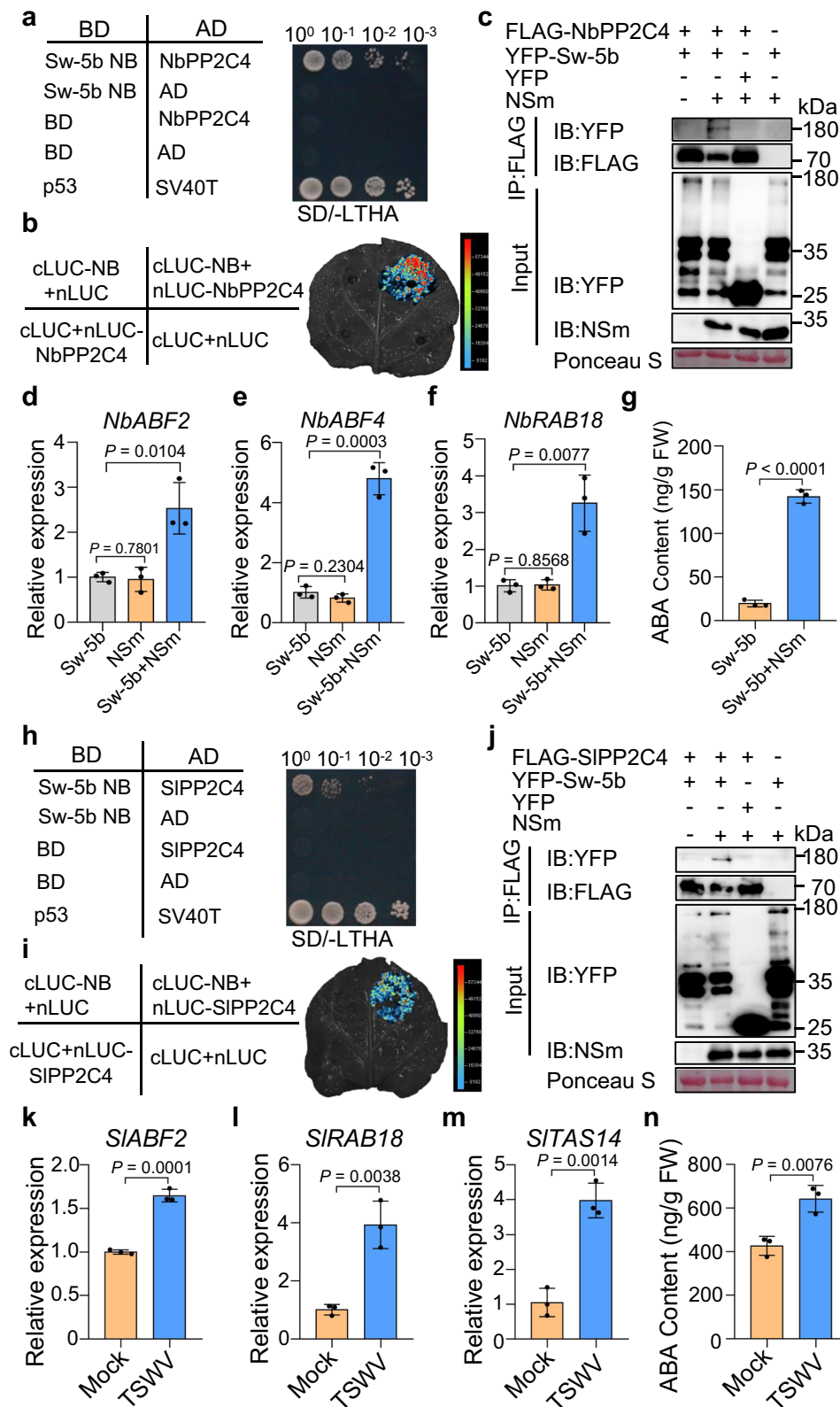
Our previous results showed that the *Sw-5b* NB domain alone could induce elicitor-independent hypersensitive response (HR) cell death⁴⁰, suggesting that this domain plays a vital role in the activation of downstream immune signaling. To resolve the underlying mechanism, we used the NB domain as “bait” and performed yeast-two hybrid (Y2H) screening using the *Nicotiana benthamiana* cDNA library to identify the host proteins that interact with the *Sw-5b* NB domain. We identified 35 proteins as potential candidates, including SGT1, which has been shown to interact with other NLRs⁴¹. Among the selected NB-interacting proteins, one encoded *NbPP2C4* (Supplementary Table 1), a homolog of group A PP2C-type protein phosphatase (Supplementary Fig. 1) in *Arabidopsis* that functions in ABA signaling²². Y2H and split luciferase complementation (SLC) assays confirmed that *Sw-5b* NB interacts with *NbPP2C4* (Fig. 1a, b and Supplementary Fig. 2a). To test whether the interaction of NB with *NbPP2C4* can activate ABA signaling, we transiently expressed *Sw-5b* NB in *N. benthamiana* leaves. The

results showed that the representative ABA response genes were significantly upregulated upon expression of the *Sw-5b* NB domain (Supplementary Fig. 3a–c). ABA hormone levels were also significantly increased in plant leaves expressing *Sw-5b* NB (Supplementary Fig. 3d). The co-immunoprecipitation (Co-IP) assay results also showed that the full-length *Sw-5b* associated with the *NbPP2C4* protein only in the presence of the viral effector NSm (Fig. 1c). However, *Sw-5b* mutant with NB domain deletion did not interact with *NbPP2C4* (Supplementary Fig. 4a). Consistently, the auto-active *Sw-5b*^{D857V} mutant⁴² interacted with the *NbPP2C4* protein in the absence of NSm (Supplementary Fig. 4b). A quantitative reverse-transcription polymerase chain reaction (qRT-PCR) assay further demonstrated that the relative expression levels of ABA response genes were strongly upregulated in leaves co-expressing *Sw-5b* and NSm, but not in those expressing *Sw-5b* or NSm alone (Fig. 1d–f). ABA hormone levels were also significantly increased in plant leaves co-expressing *Sw-5b* and NSm (Fig. 1g). These data suggest that *Sw-5b* activates ABA signaling upon recognition of the viral effector NSm. We use tobacco rattle virus (TRV)-mediated gene silencing to knock down *NbABA2* and disrupt the ABA biosynthesis in *N. benthamiana* (Supplementary Fig. 5a–c), followed by co-expression of *Sw-5b* and NSm. The results showed that despite ABA biosynthesis is disrupted, co-expression of *Sw-5b* and NSm still significantly upregulates the ABA response genes (Supplementary Fig. 5d–f). The expression levels of the ABA response genes induced by *Sw-5b* in the *NbABA2*-silenced plants are lower than those in the non-silenced control plants (Supplementary Fig. 5d–f). *Sw-5b* localizes in both cytoplasm and nucleus⁴³. To investigate which sub-cellular pools of *Sw-5b* can induce the ABA responses, we co-expressed NES-*Sw-5b* and NLS-*Sw-5b* with NSm in *N. benthamiana* leaves. The results showed that both the cytoplasmic and nuclear pools of the *Sw-5b* NLR can induce ABA response genes in the presence of NSm, whereas the nuclear pools of the *Sw-5b* induce slightly higher levels of ABA response genes than the cytoplasmic pools (Supplementary Fig. 6a–c).

Next, we examined the interaction between *Sw-5b* NB and *S/PP2C4* from tomato plants. The results of Y2H, Co-IP, and SLC assays showed that *Sw-5b* NB interacted with *S/PP2C4* in vitro and in planta (Fig. 1h, i and Supplementary Figs. 2b, 7). The full-length *Sw-5b* was also associated with *S/PP2C4* protein, but only in the presence of the viral NSm (Fig. 1j). The results of qRT-PCR assay further showed that the expression levels of the ABA response genes were significantly upregulated in tomato cv. IVF3545 plants (with *Sw-5b* gene) inoculated with TSWV (Fig. 1k–m). ABA levels were also significantly increased upon recognition of TSWV in tomato cv. IVF3545 plants (Fig. 1n). We also silenced *SLABA2* to inhibit ABA biosynthesis in tomato cv. IVF3545 plants (Supplementary Fig. 8a–c), followed by TSWV inoculation. TSWV inoculation still upregulates the ABA response genes in *SLABA2*-silenced plants compared to the mock-inoculated control plants (Supplementary Fig. 8d–f).

Knockout/down *NbPP2C4/SIPP2C4* activates ABA-mediated defense against TSWV infection in *N. benthamiana* and tomato plants

As *Sw-5b* activates ABA signaling pathways, we first examined whether ABA signaling can provide a defense against TSWV infection. Wild-type (WT) *N. benthamiana* and tomato plants were treated with 100 μM ABA and mechanically inoculated with TSWV. Plants treated with 0.2% EtOH were used as a control. The results showed that disease symptoms and viral accumulation were significantly reduced in systemic leaves of WT *N. benthamiana* and tomato plants by ABA treatment (Fig. 2a–d and Supplementary Fig. 9a, b), suggesting that exogenous application of ABA induces defense against TSWV infection. To further investigate whether ABA-induced defense inhibits the replication or intercellular movement of TSWV, the leaves of *N. benthamiana* plants were treated with 100 μM ABA, followed by the inoculation of the



TSWV S segment-based minireplicon carrying eGFP reporter [SR⁽⁺⁾ eGFP] which can replicate only or the expression of the NSm movement protein::GFP fusion protein (NSm-GFP) which can move from one cell to other cells⁴³⁻⁴⁵. The results showed that ABA treatment not only inhibited the replication, but also disrupted the intercellular movement of TSWV (Supplementary Fig. 10a-d).

To further characterize PP2C4 in the ABA signaling pathway against viral infection, we generated two independent knockout mutant lines, *Nbpp2c4-5* and *Nbpp2c4-10*, using CRISPR-Cas9-based gene editing technology (Supplementary Fig. 11a, b). *Nbpp2c4-5* and *Nbpp2c4-10* mutants were more sensitive to ABA treatment in both seed germination and primary root growth inhibition assays compared

Fig. 1 | Sw-5b NLR interacts directly with PP2C4 and activates ABA responses. **a** Y2H assay of the interaction between Sw-5b NB and NbPP2C4. AD activation domain. BD DNA binding domain. BD-P53 and AD-SV40T were used as positive controls. Protein interaction was assayed on SD/-LTHA dropout media. Yeast cell growth in SD/-LT dropout media is shown in Supplementary Fig. 2a. **b** SLC assay of the interaction between Sw-5b NB and NbPP2C4 at 48 h post-infiltration (hpi). **c** Co-IP analysis of the interaction between Sw-5b and NbPP2C4 with or without NSm. Proteins in blots were detected with FLAG-, YFP-, or NSm-specific antibodies. Ponceau S staining was performed to determine the amount of protein load. The protein size marker is shown to the right. **d–f** Relative expression levels of *NbABF2*, *NbABF4*, and *NbRAB18* in *N. benthamiana* leaves by (co)expressing Sw-5b, NSm or both. **g** Amount of ABA in *N. benthamiana* leaves (co)expressing Sw-5b or Sw-5b

and NSm. The exact *P* value is provided in the Source Data. **h** Y2H assay for the protein interaction between Sw-5b NB and *SIPP2C4* on SD/-LTHA dropout medium. Yeast cell growth in SD/-LT dropout media is shown in Supplementary Fig. 2b. **i** SLC analysis of the interaction between Sw-5b NB and *SIPP2C4* at 48 hpi. **j** Co-IP analysis of the interaction between Sw-5b and *SIPP2C4*. **k–m** Relative expression levels of *SIABF2*, *SIRAB18*, and *SITAS14* in tomato plant (+*Sw-5b*) leaves inoculated with TSWV at 4 dpi. *SIActin* was used as the internal reference gene. Plants inoculated with phosphate buffer (PB) were used as a Mock control. **n** Amount of ABA in tomato plant (+*Sw-5b*) leaves inoculated with TSWV at 4 dpi. **d–g, k–n** Data were presented as means \pm s.d. ($n = 3$ biologically independent samples). Data were analysed by two-sided Student's *t*-test. Source data are provided as a Source Data file. All experiments were repeated at least three times with similar results.

to WT *N. benthamiana* plants (Fig. 2e and Supplementary Fig. 12a–c). Consistently, the expression levels of ABA response genes *NbABF2*, *NbABF4*, and *NbRAB18* (ABF, ABA-responsive element binding factor) were greatly elevated in *Nbpp2c4* plants compared with those in WT plants, in response to ABA treatment (Fig. 2f and Supplementary Fig. 13a).

Next, we inoculated two *Nbpp2c4* mutant lines and WT *N. benthamiana* plants with TSWV infectious clones ($L_{opt(+)}M_{opt(-)}SR_{(+)}eGFP$) carrying enhanced green fluorescent protein (eGFP) reporter via agroinfiltration⁴⁴. Compared to the WT control plants, the *Nbpp2c4-5* and *Nbpp2c4-10* mutant lines accumulated much less eGFP fluorescence expressed from the TSWV replicon (Supplementary Fig. 14a, b). The *Nbpp2c4-5* and *Nbpp2c4-10* mutants were also mechanically inoculated with TSWV-infected leaf extracts, resulting in a significant reduction in disease symptoms and TSWV accumulation compared to the WT control plants (Fig. 2g, h). To investigate whether this effect was specific to TSWV, the leaves of *Nbpp2c4-5* and *Nbpp2c4-10* mutants were also inoculated with an infectious clone of potato virus X carrying a GFP reporter (PVX-GFP) and potato virus Y carrying a GFP reporter (PVY-GFP), respectively, by agroinfiltration. The results showed that both PVX-GFP and PVY-GFP accumulated significantly less in *Nbpp2c4-5* and *Nbpp2c4-10* mutants than those in WT plants (Supplementary Fig. 15a–d), suggesting that *Nbpp2c4* knockout also reduces the infection of other viruses.

We also silenced *SIPP2C4* in cv. Moneymaker (without *Sw-5b*) using TRV-based virus-induced gene silencing (VIGS). The expression levels of ABA response genes *SIABF2*, *SIRAB18*, and *SITAS14* were significantly higher in *SIPP2C4*-silenced tomato plants than those in TRV-GUS control plants in response to ABA treatment (Fig. 2i and Supplementary Fig. 13b–d). *SIPP2C4*-silenced tomato plants were also mechanically inoculated with TSWV-infected leaf extracts. As shown in Fig. 2j, k, disease symptoms and viral accumulation were significantly reduced in systemic leaves of *SIPP2C4*-silenced tomato plants compared to control plants. Together, these results suggest that *NbPP2C4/SIPP2C4* plays a negative role in the ABA response, and knockout/down *NbPP2C4/SIPP2C4* activates the ABA-mediated defense against TSWV infection in *N. benthamiana* and tomato plants.

Overexpression of SnRK2.3/2.4 induces ABA-dependent immunity to TSWV, and their function is inhibited by PP2C4

SnRK2s are critical for ABA signal transduction³¹. Among ten *SnRK2*s in *Arabidopsis*, *AtSnRK2.3*, *AtSnRK2.4*, and *AtSnRK2.6* are the major *SnRK2* genes that participate in regulating ABA signaling⁴⁶. *NbSnRK2.3/2.4* and *SISnRK2.3/2.4* from *N. benthamiana* and tomato are the closest homologs to *AtSnRK2.3/2.4/2.6* (Supplementary Fig. 16a). Transient overexpression of *NbSnRK2.3/2.4* or *SISnRK2.3/2.4* upregulated the expression of representative ABA response genes (Fig. 3a and Supplementary Fig. 17a–d). Consistently, the expression levels of *NbSnRK2.3* and *NbSnRK2.4* with TSWV infectious clones also inhibited eGFP expression from the TSWV replicon in WT *N. benthamiana* leaves (Fig. 3b). Similar results were observed for the expression levels of *SISnRK2.3* and *SISnRK2.4* with the TSWV replicon (Supplementary

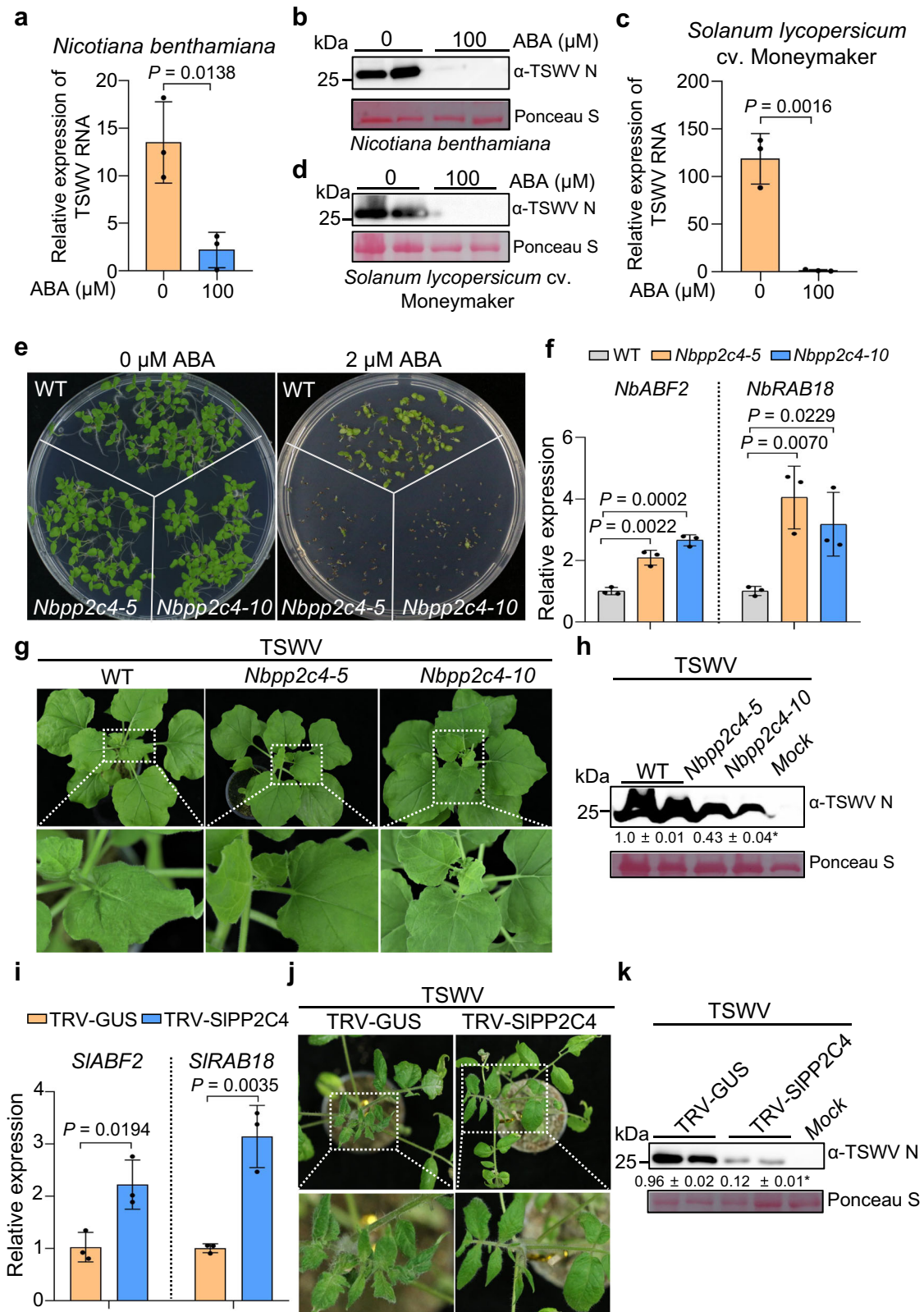
Fig. 18a). The inhibition of TSWV accumulation by *SnRK2.3/SnRK2.4* was further confirmed by immunoblotting (Fig. 3c and Supplementary Fig. 18b). However, silencing *NbSnRK2.3* and *NbSnRK2.4* using TRV-based VIGS was lethal to *N. benthamiana* plants (Supplementary Fig. 19), which suggests that *NbSnRK2.3* and *NbSnRK2.4* are required for plant development and growth. Alternatively, we knocked down *NbSnRK2.3/2.4* by transient expression of double-stranded hairpin RNA (double-stranded RNA interference [dsRNAi]), which targeted the mRNA of both *NbSnRK2.3* and *NbSnRK2.4* in WT *N. benthamiana* leaves. Compared with dsGUS control, leaves treated with ds*NbSnRK2.3/2.4* had much higher eGFP expression from the TSWV replicon (Fig. 3d–f), suggesting that *NbSnRK2.3/2.4* play a positive role in the defense against TSWV.

We also investigated the role of *NbSnRK2.3/2.4* in Sw-5b-mediated resistance against TSWV. When leaf halves from *NbSnRK2.3/2.4*-suppressed or non-suppressed Sw-5b transgenic *N. benthamiana* plants were rub-inoculated with TSWV-infected leaf extracts, TSWV inoculation induced significantly more HR loci in *NbSnRK2.3/2.4*-suppressed leaf halves than in non-suppressed leaf halves (Fig. 3g, h). Analysis of TSWV-inoculated leaves through immunoblotting further showed that the accumulation level of viral nucleocapsid protein in TSWV-inoculated *NbSnRK2.3/2.4*-suppressed leaf halves was significantly higher than that in TSWV-inoculated non-suppressed leaf halves (Fig. 3i). To further investigate whether suppression of *NbSnRK2.3/2.4* would affect the induction of cell death, we knocked down *NbSnRK2.3/2.4* by transient expression of double-stranded hairpin RNA, followed by co-expression of Sw-5b and NSm. We also treated *N. benthamiana* leaves with 100 μ M ABA as a control. The results showed that neither *NbSnRK2.3/2.4* knockdown nor ABA treatment affected cell death (Supplementary Fig. 20a–d).

The Y2H assay result showed that *NbPP2C4* interacted with *NbSnRK2.3* and *NbSnRK2.4*, respectively (Supplementary Fig. 16b). Next, we tested whether *NbPP2C4* could inhibit the function of *NbSnRK2.3/2.4* in activating immunity to TSWV by co-expressing TSWV infectious clones carrying eGFP reporter with *NbSnRK2.3/2.4* and empty vector (EV) control or *NbSnRK2.3/2.4* and *NbPP2C4* in *N. benthamiana* leaves. Compared to the low GFP accumulation in the *NbSnRK2.3/2.4*+EV control group, co-expression of *NbSnRK2.3/2.4* with *NbPP2C4* significantly increased TSWV accumulation (Fig. 3j, k). Similar results were observed by comparing the effects of *SISnRK2.3/2.4* and EV with *SISnRK2.3/2.4* and *SIPP2C4* (Supplementary Fig. 21). These results suggest that *NbPP2C4* inhibits the function of *NbSnRK2.3/2.4* in activating the host defense against TSWV.

Sw-5b NLR releases SnRK2.3/2.4 from PP2C4 inhibition via the NB domain to activate antiviral immunity

Given that the ABA-receptor complex PYR/PYL/RCAR in the presence of ABA binds to PP2C and depresses PP2C repression of SnRK2s-mediated activation of ABA signaling⁴⁷, we hypothesized that Sw-5b NB may function in a similar manner to that of the ABA receptor and that binding to PP2C4 may interfere with the interaction between PP2C4 and SnRK2s. Yeast three-hybrid (Y3H) assay results showed that



interaction between NbPP2C4 and NbSnRK2.3/NbSnRK2.4 was reduced significantly in the presence of Sw-5b NB compared to the yellow fluorescent protein (YFP) control (Fig. 4a). Glutathione S-transferase (GST) pull-down assays also showed that when the amount of YFP-Sw-5b-NB increased, the amount of FLAG-NbPP2C4 pulled down by GST-NbSnRK2.3/2.4 decreased (Fig. 4b, c). The same

assay showed that the addition of His-YFP had no effect on the interaction between FLAG-NbPP2C4 and GST-NbSnRK2.3/2.4 (Fig. 4b, c).

SIPP2C4 also interacted with SISnRK2.3 and SISnRK2.4, respectively, in yeast (Supplementary Fig. 16c). The Y3H assay results showed that the interaction between SIPP2C4 and SISnRK2.3/SISnRK2.4 was strongly compromised in the presence of Sw-5b NB, but not YFP

Fig. 2 | Knockout/down *NbPP2C4/SIPP2C4* activates ABA-dependent defense against TSWV infection in *N. benthamiana* and tomato plants. **a** Relative expression levels of TSWV RNAs in *N. benthamiana* plants with or without 100 μ M ABA treatment. **b** Immunoblot analysis of TSWV accumulation in *N. benthamiana* plants with or without ABA treatment using viral N protein-specific antibodies. **c** Relative expression levels of TSWV RNAs in tomato plants (*-Sw-5b*) with or without ABA treatment. **d** Immunoblot analysis of TSWV accumulation in tomato plants (*-Sw-5b*) treated with or without ABA treatment. **e** Seed germination of *Nbpp2c4-5* and *Nbpp2c4-10* knockout mutants is inhibited in the presence of 2 μ M ABA compared to wild-type (WT) *N. benthamiana* plants. Seeds were germinated on MS medium without ABA (left) or with 2 μ M ABA (right) for 10 days. **f** Expression levels of *NbABF2* and *NbRAB18* in *Nbpp2c4-5* or *Nbpp2c4-10* mutant plants were significantly higher than that in WT *N. benthamiana* plants in response to ABA (100 μ M). **g** Phenotypes of WT, *Nbpp2c4-5*, and *Nbpp2c4-10* mutant plants

inoculated with TSWV photographed at 7 dpi. **h** Immunoblot analysis of TSWV accumulation in systemic leaves of WT, *Nbpp2c4-5*, and *Nbpp2c4-10* plants using viral N protein-specific antibodies. Plants inoculated with PB buffer were used as Mock controls. **i** Expression levels of *SLABF2* and *SIRAB18* in *SIPP2C4*-silenced tomato plants are significantly higher than those in TRV-*GUS* control plants in response to ABA (100 μ M) treatment. **j** Phenotypes of TRV-*GUS* or TRV-*SIPP2C4*-treated tomato plants (*-Sw-5b*) infected with TSWV were photographed at 7 dpi. **k** Immunoblot analysis of TSWV accumulation in plant leaves shown in panel **j** using viral N protein-specific antibodies. Plants inoculated with PB were used as Mock controls. Ponceau S staining was used to determine the amount of protein loading. **a, c, f, i** Data were presented as means \pm s.d. ($n = 3$ biologically independent samples). *P* values are indicated in the graphs or Source Data (two-sided Student's *t*-tests). **b, d, h, k** Experiments were repeated at least three times with similar results. Source data are provided as a Source Data file.

(Supplementary Fig. 22a). GST pull-down assays confirmed that the interaction between *SIPP2C4* and *SlSnRK2.3/SlSnRK2.4* was reduced significantly with an increase in the amount of YFP-Sw-5b-NB; however, this interaction was not affected by the presence of YFP (Supplementary Fig. 22b, c).

Because Sw-5b NLR interacts with NbPP2C4 upon recognition of the viral effector NSm (Fig. 1), we investigated whether Sw-5b NLR can depress *NbPP2C4* inhibition of *NbSnRK2.3/2.4* during viral infection. We co-expressed TSWV infectious clones with *NbSnRK2.3/2.4* and *NbPP2C4*, or *NbSnRK2.3/2.4*, *NbPP2C4* and *Sw-5b* in *N. benthamiana* leaves. Compared to the high level of GFP accumulation attained by co-expression of *NbSnRK2.3/2.4* and *NbPP2C4*, the addition of Sw-5b to the *NbSnRK2.3/2.4*-*NbPP2C4* complex significantly inhibited TSWV accumulation (Fig. 4d, e). Next, we co-expressed TSWV SR₍₊₎eGFP minireplicon with *NbSnRK2.3/2.4* and *NbPP2C4* in the presence of *EV*, *Sw-5b*, or *Sw-5b + NSm* in *N. benthamiana* leaves. The results showed that the co-addition of Sw-5b with only the NSm effector inhibited the accumulation of TSWV SR₍₊₎eGFP minireplicon (Supplementary Fig. 23a–d). We also co-expressed TSWV infectious clones with *SlSnRK2.3/2.4* and *SIPP2C4*, or *SlSnRK2.3/2.4*, *SIPP2C4* and *Sw-5b* in *N. benthamiana* leaves. Similar effects were observed (Supplementary Fig. 24a, b). These results suggest that Sw-5b depresses PP2C repression of *SnRK2.3/2.4* and activates a strong defense against TSWV.

Sw-5b NLR induces stomatal closure and drought resistance in *N. benthamiana* and tomato plants upon recognition of the viral effector NSm

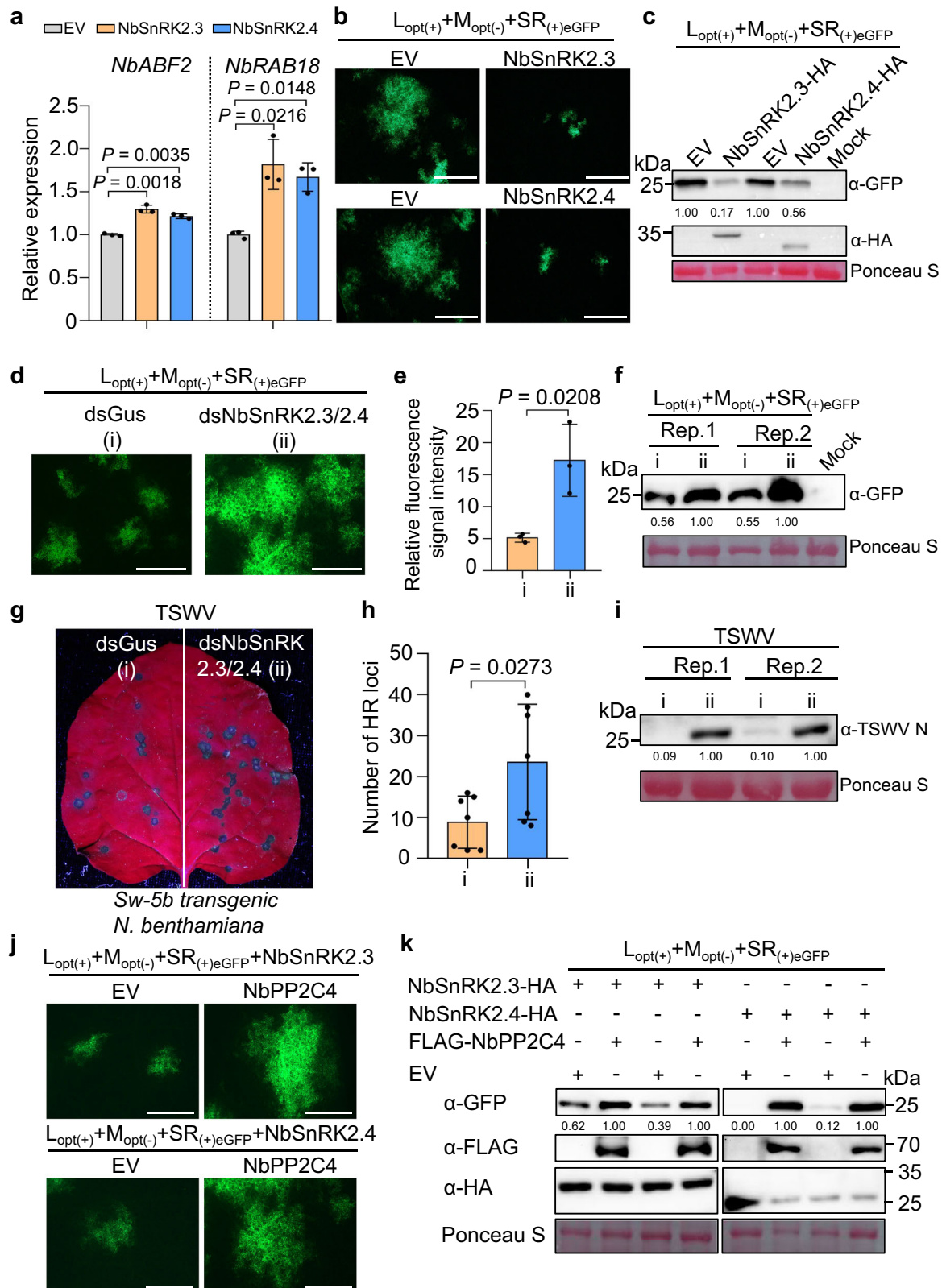
Because co-expression of Sw-5b and NSm induced ABA signaling, we examined whether Sw-5b NLR induces stomatal closure in the presence of NSm. When Sw-5b was co-expressed with the viral effector NSm in *N. benthamiana* leaves, stomatal closure was frequently detected (Fig. 5a, b). However, this effect was not observed in leaves expressing Sw-5b or NSm alone. When *NbSnRK2.3/2.4* was knocked down, co-expression of Sw-5b and NSm did not lead to activation of ABA response genes and induction of stomatal closure (Supplementary Fig. 25a–e), suggesting that Sw-5b induced stomatal closure depends on *NbSnRK2.3/2.4*. We also examined whether Sw-5b NLR can induce drought tolerance upon the detection of NSm. In response to drought, *Sw-5b* transgenic *N. benthamiana* plants with TSWV inoculation showed significantly enhanced drought tolerance compared with Mock-inoculated plants (Fig. 5c). In tomato plants carrying the *Sw-5b* resistance gene, stomatal closure was also frequently detected in TSWV-inoculated leaves compared with mock-inoculated plant leaves (Fig. 5d, e), and drought tolerance was significantly enhanced in TSWV-inoculated tomato plants carrying *Sw-5b* (Fig. 5f). These results suggest that Sw-5b NLR not only induces ABA-dependent immunity to viral infection but also promotes drought resistance in plants upon recognition of the viral effector protein.

Discussion

In this study, we demonstrated that Sw-5b NLR behaves in a similar manner as ABA receptors and directly employs the PP2C-SnRK2 complex, the central regulator of ABA signaling, to activate antiviral immunity. We show that pathogen effector recognition by Sw-5b NLR induces ABA-dependent antiviral signaling. The NB domain of Sw-5b NLR directly interacts with group A NbPP2C4/SIPP2C4 from *N. benthamiana* and tomato plants. Group A NbPP2C4/SIPP2C4 interacts with and inhibits *NbSnRK2.3/2.4* or *SlSnRK2.3/2.4*. Knockout/down PP2C4 or overexpression of *SnRK2.3/2.4* activates the ABA-specific defense pathway against TSWV infection in *N. benthamiana* or in tomato plants. Upon recognition of viral effector NSm, the Sw-5b NLR undergoes conformational changes that allow binding to PP2C4 via the NB domain. This NLR receptor-PP2C binding interferes with the interaction between PP2C4 and *SnRK2.3/2.4*, thereby releasing *SnRK2.3/2.4* from PP2C4-mediated inhibition to activate the ABA-dependent defense against viral pathogens. Meanwhile, Sw-5b NLR-induced stomatal closure and drought resistance in *Nicotiana benthamiana* and tomato plants. These findings provide important insights into the activation of hormone signaling pathways by plant immune receptors.

The phytohormone ABA plays a pivotal role in plant defenses against viruses⁴⁸. In this study, we found that Sw-5b NLR induces ABA accumulation and up-regulation of ABA response genes upon recognition of viral effector NSm. Exogenous application of ABA induces plant defense against TSWV infection. Consistently, knockout/down NbPP2C4/SIPP2C4 or overexpression of *SnRK2.3/2.4* activates the ABA signaling-dependent defense against tospoviral infection (Fig. 2). These data suggest that the ABA signaling pathway activated by Sw-5b NLR plays a key role in plant defense against viral pathogens. Soybean NLR Rsv3-mediated extreme resistance against SMV was also found to induce ABA accumulation and downstream ABA signaling²⁰. ABA was able to prime callose deposition and inhibit viral cell-to-cell movement³⁸. The Sw-5b NLR-induced defense was also able to inhibit viral intercellular movement⁴³. Activation of the ABA signaling pathway by both tomato Sw-5b and soybean Rsv3 NLRs suggests that ABA has an important antiviral role and that this signaling pathway can be employed by both NLRs to defend against viral infection.

Not only effector NSm recognition by Sw-5b NLR induces ABA accumulation and signaling, but also Sw-5b NB alone can induce ABA accumulation and signaling. Using Y2H screening, GST pull-down, co-IP, and SLC assays, we found that the Sw-5b NB domain directly interacts with group A NbPP2C4/SIPP2C4 from *N. benthamiana* and tomato plants (Fig. 1). Group A PP2Cs act in a negative feedback regulatory loop of the ABA signaling pathway^{21,27,49}. Genetically, knockout/down *NbPP2C4/SIPP2C4* was more sensitive to ABA treatment. Meanwhile, the expression of ABA marker genes was much higher in *pp2c4* knockout mutants than in WT in response to ABA (Fig. 2), suggesting that *NbPP2C4/SIPP2C4* from *N. benthamiana* and tomato plants has a



similar function to group A PP2Cs from *Arabidopsis* in ABA signaling. In *Arabidopsis*, PP2Cs physically interacted with SnRK2s and inactivated SnRK2³⁰. Our Y2H and GST pull-down assays showed that NbPP2C4/SIPP2C4 interacts with and inhibits the function of NbSnRK2.3/4 or SlSnRK2.3/2.4 (Fig. 4a–c and Supplementary Fig. 22). SnRK2s are key regulators of ABA signaling transduction in *Arabidopsis*⁴⁶. We found that overexpression of NbSnRK2.3/2.4 or

SlSnRK2.3/2.4, the orthologs of SnRK2s in *Arabidopsis*, significantly upregulated the expression of ABA-responsive genes (Fig. 3a and Supplementary Fig. 17), suggesting that SnRK2.3/2.4 from *N. benthamiana* and tomato plants play an important role in ABA signaling. Furthermore, the downregulation of SnRK2.3/2.4 reduces the Sw-5b-mediated disease resistance against virus infection, suggesting that SnRK2.3/2.4-mediated ABA signaling is required for Sw-5b to confer

Fig. 3 | Overexpression of SnRK2.3/2.4 induces ABA-dependent immunity to TSWV, and their function is inhibited by PP2C4. **a** Relative expression levels of *NbABF2* and *NbRAB18* in *N. benthamiana* leaves transiently overexpressing *NbSnRK2.3/2.4* at 24 h post-agroinfiltration (hpa). EV, p2300S empty vector. **b** Overexpression of *NbSnRK2.3/2.4* inhibits TSWV replicon accumulation in *N. benthamiana* plants. The eGFP fluorescence expressed from TSWV replicon ($L_{(-)opt}$, $M_{(-)opt}$, and $SR_{(+),eGFP}$) was examined using an inverted fluorescence microscope at 2.5 dpi. Bars = 800 μ m. **c** Immunoblot analysis of TSWV accumulation in *N. benthamiana* leaves expressing *NbSnRK2.3/2.4*-HA using GFP and HA-specific antibodies, respectively. Mock, plant leaves treated with EV. **d** Silencing *NbSnRK2.3/2.4* enhanced TSWV accumulation in *N. benthamiana* leaves. The eGFP fluorescence expressed from the TSWV replicon was examined at 2.5 dpi. Bars = 800 μ m. **e** Relative fluorescence signal intensity in leaves shown in panel **d** quantified using ImageJ software. **f** Immunoblot analysis of TSWV replicon accumulation in leaves shown in panel **d** with GFP-specific antibodies. **g** Silencing *NbSnRK2.3/2.4* reduced

Sw-5b-mediated resistance against TSWV in *N. benthamiana* plants. *Sw-5b* transgenic *N. benthamiana* plants treated with double-strand RNA targeting *NbSnRK2.3/2.4* (ds*NbSnRK2.3/2.4*) or with dsGus control were mechanically inoculated with TSWV-infected leaf sap. HR loci induced in inoculated leaves were monitored and photographed at 3 dpi. **h** Statistical analysis of HR loci treated with ds*NbSnRK2.3/2.4* or dsGus control in panel **g**. **i** Immunoblot analysis of TSWV accumulation in inoculated leaves shown in panel **g** using viral N protein-specific antibodies. **j** Overexpression of *SnRK2.3/2.4* induces ABA-dependent immunity to TSWV, and their function is inhibited by PP2C4. The eGFP expressed from the TSWV replicon was examined at 2.5 dpi. Bars = 800 μ m. **k** Immunoblot analysis of TSWV accumulation in panel **j** using GFP, FLAG, and HA-specific antibodies, respectively. Ponceau S staining was used to determine the amount of protein loading. **a, e** Data were presented as means \pm s.d ($n = 3$); **h, j** $n = 7$. *P* values are shown in the graphs (two-sided Student's *t*-test). Source data are provided as a Source Data file. All experiments were repeated at least three times with similar results.

full immunity. Importantly, Sw-5b NB interferes with the interaction between PP2C4 and SnRK2.3/2.4, thereby activating the SnRK2.3/2.4 to initiate the ABA signaling pathway in *N. benthamiana* and tomato plants to defend against TSWV.

We found that Sw-5b NLR interacts strongly with PP2C4 only when Sw-5b recognizes the viral effector NSm (Fig. 1), suggesting that the NB domain of Sw-5b NLR undergoes a major conformational change upon effector recognition and allowing NB binding to PP2C4. In our previous studies, we showed that the binding of the effector NSm onto the four polymorphic sites of the Sw-5b LRR domain interferes with the adjacent R927 residue and disrupts the intramolecular interaction between the NB and LRR domains, which in turn causes the conformational change of NB domain, thereby switching the Sw-5b immune receptor from an inactive state to an active state³⁷. In the recently resolved 3D cryo-electron microscopy structure of the inactive and active states of the *Arabidopsis* NLR ZARI, a key difference between the inactive and active states of ZARI is the conformational change in the NB domain⁵⁰. The Sw-5b NB domain interacted directly with PP2C4 and the full-length of Sw-5b Sw-5b interacted with PP2C4 only in the presence of NSm. Our results, together with previous findings, suggest that the NB domain of Sw-5b undergoes a conformational change from an inactive state to an activated state upon effector recognition, and only with this activated conformation can Sw-5b NB associate with PP2C and activate the ABA signaling pathway.

Sw-5b plants exhibited significantly better drought tolerance with TSWV inoculation. Thus, as tomato plants evolve to the point of acquiring Sw-5b NLR, they may simultaneously acquire drought resistance capability. This hypothesis has important implications, in that Sw-5b NLR, a disease-resistance gene, may play both a virus-resistance role and a previously unknown role in drought resistance. Notably, plants carrying NLR experience a growth penalty, with ~5% yield loss⁵¹ due to low levels of auto-activation of NLR. It is not known whether plants become more drought-tolerant when NLRs are introduced to plants. Whether Sw-5b or other NLRs are involved in both disease resistance and drought resistance, and whether these NLRs will be useful in breeding for both disease- and drought-resistant lines, are research avenues worthy of further exploration.

Based on the findings described above, we proposed a working model that Sw-5b, an NLR receptor of the plant innate immune system, mimics the behavior of the ABA receptors and directly modulates the ABA central regulator PP2C4-SnRK2 complex to activate ABA-dependent antiviral immunity (Fig. 6). At the center of the ABA signaling regulation, PP2C interacts with and constitutively inhibits SnRK2 function in the absence of ABA, whereas upon detection of ABA, the ABA receptor PYLs undergo a conformational change that enables binding to PP2C. The ABA-receptor binding releases SnRK2 from PP2C-mediated inhibition, thereby allowing SnRK2 to activate ABA signaling. The Sw-5b NLR immune receptor behaves in a similar manner to ABA receptors. In the absence of the viral effector NSm, Sw-5b NLR is

maintained in an inactive state. Upon recognition of the effector NSm, Sw-5b NLR switches from an inactive to an active conformation that allows binding to PP2C4 via the NB domain. The NLR-PP2C binding interferes with the interaction between PP2C4 and SnRK2.3/2.4 and releases SnRK2s from PP2C4 inhibition, thereby activating ABA-dependent antiviral immunity.

Methods

Plant material and growth conditions

The 6-to-8-week-old *Nicotiana benthamiana* plants were used for viral infection clone inoculation, protein analyses, and other experiments. The source of *Sw-5b* transgenic *N. benthamiana* lines has been described previously⁴². *Nbpp2c4* knockout *N. benthamiana* mutant lines were generated using a CRISPR/Cas9-based technology in this lab. T2 transgenic lines were used in this study. Seeds of tomato cv. '1VF3545' carrying the *Sw-5b* resistance gene were provided by Prof. Junming Li at the Institute of Vegetables and Flowers, Chinese Academy of Agricultural Sciences, Beijing, China. Seeds of tomato cv. 'Moneymaker' without *Sw-5b* were provided by Dr. Hui Zhang at the Institute of Horticulture Science, Shanghai Academy of Agricultural Sciences, Shanghai, China. We used 4-week-old tomato plants for VIGS assays. All *N. benthamiana* plants and tomato seedlings were grown in an environmentally controlled greenhouse under a 16-h light (25 °C)/8-h dark (23 °C) photoperiod.

Plasmid construction

The plasmids p2300S-YFP, p2300S-YFP-Sw-5b, p2300S-NSm, p2300S-Sw-5b, and p2300S-YFP-NB were described previously^{40,42}. The coding sequences of PP2C4, SnRK2.3, and SnRK2.4 from *N. benthamiana* and tomato (*Solanum lycopersicum*) were amplified by RT-PCR, fused with HA or FLAG tags in their N-terminus or C-terminus, and cloned individually into pCambia2300S under the control of the 35S promoter⁵².

To generate constructs expressing GST-SnRK2.3 and GST-SnRK2.4, their coding sequences were amplified by PCR and cloned into the pGEX-2TK vector. FLAG-PP2C4, YFP, and YFP-NB were cloned into pET-28a to generate pET-28a-FLAG-PP2C4, pET-28a-YFP, and pET-28a-YFP-NB, respectively.

AD-PP2C4, BD-SnRK2.3, BD-SnRK2.4, and BD-Sw-5b-NB were amplified by PCR and cloned into pGADT7 or pGBKT7. To generate the constructs BD-SnRK2.3-NB/YFP and BD-SnRK2.4-NB/YFP for the Y3H assays, Sw-5b-NB and YFP were amplified by PCR and cloned into a pBridge vector (Clontech, Mountain View, CA, USA) driven by a MET25 promoter. Subsequently, SnRK2.3 and SnRK2.4 were cloned into pBridge-NB/YFP, respectively.

The constructs for creating *Nbpp2c4* CRISPR-Cas9 knockout lines were generated by inserting a small guide RNA oligomer into the binary vector BGK01⁵³. The synthesized sgRNA oligomers were annealed and then ligated to BGK01 with T4 DNA ligase to generate BGK01-NbPP2C4.

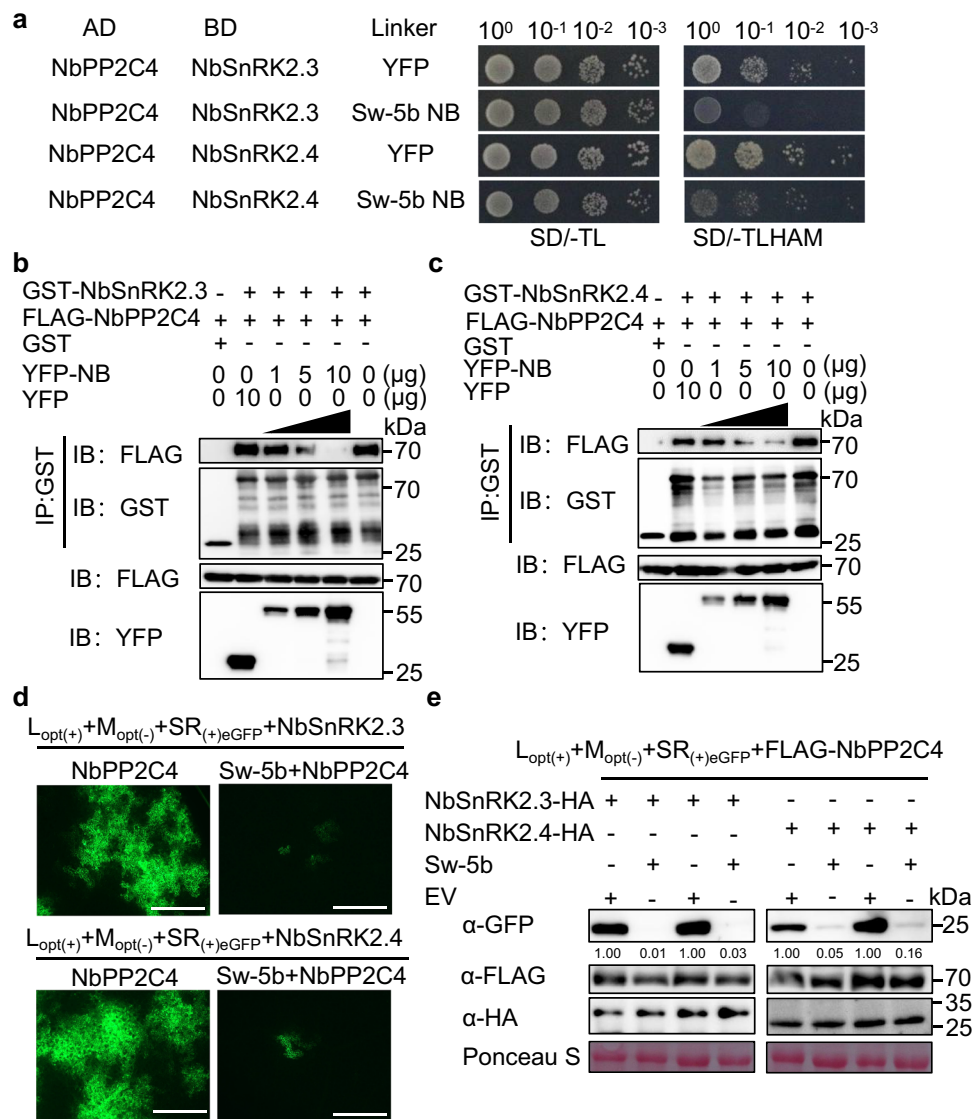


Fig. 4 | Sw-5b NLR depresses PP2C4 repression of SnRK2.3/2.4 via the NB domain to activate ABA-dependent defense against TSWV. **a** Yeast three-hybrid (Y3H) assays showing the effect of Sw-5b NB on the interaction between *NbPP2C4* and *NbSnRK2.3* or between *NbPP2C4* and *NbSnRK2.4*. Yeast cells were co-transformed with pGAD-*NbPP2C4* and pBridge-*NbSnRK2.3/2.4* + YFP or pGAD-*NbPP2C4* and pBridge-*NbSnRK2.3/2.4* + Sw-5b NB domain. The interactions were assayed on SD/-TL (lacking Trp and Leu) and SD/-TLHAM (lacking Trp, Leu, His, Ade, and Met) dropout medium plates, respectively, for 3–5 days. **b**, **c** Glutathione S-transferase (GST) pull-down assays to assess Sw-5b NB interference with interaction between *NbPP2C4* and *NbSnRK2.3/2.4* in vitro. Purified GST-*NbSnRK2.3* (**b**) or GST-*NbSnRK2.4* (**c**) protein was used to pull down the FLAG-*NbPP2C4* with the

increasing amount of YFP-Sw-5b NB. YFP was used as a negative control. Blots were detected with FLAG, GST, and YFP-specific antibodies. The protein size marker is shown on the right. **d** TSWV L_{(+)opt} + M_{(-)opt} + SR_{(+)eGFP} replicons with *NbSnRK2.3* and *NbPP2C4* (upper) or *NbSnRK2.4* and *NbPP2C4* (lower) were co-expressed with Sw-5b in *N. benthamiana* leaf halves. These combinations were also co-expressed with a p2300S EV in the other half of each leaf, which were used as controls. The eGFP fluorescence expressed from the TSWV replicon was examined and photographed under an inverted fluorescence microscope at 2.5 dpi. Bars = 800 μm. **e** Immunoblot analyses of TSWV replicon accumulation shown in panel **d** using GFP, FLAG, and HA-specific antibodies, respectively. All experiments were repeated at least three times with similar results.

To knock down SIPP2C4 in tomato plants, 300 bp of the coding sequence SIPP2C4 was cloned into pTRV2 to generate pTRV2-SIPP2C4. To knock down *NbSnRK2.3* and *NbSnRK2.4* simultaneously in *N. benthamiana* plants, partial sequences (250 bp) of *NbSnRK2.3* and *NbSnRK2.4* cDNAs were amplified by RT-PCR. The resulting fragments were fused together by overlap PCR and cloned into pTRV2 to produce pTRV2-*NbSnRK2.3/2.4*. To transiently silence *NbSnRK2.3/2.4* genes by double-strand RNA in *N. benthamiana* leaves, the *NbSnRK2.3/2.4* fused fragment was forward-inserted into the p2300s-intron vector cut with *Xba* I and *Pst* I restriction enzymes. The obtained construct was then reverse-inserted with an *NbSnRK2.3&2.4* fusion fragment using *Kpn* I and *Bam* H I to generate p2300S-ds*NbSnRK2.3/2.4*.

To generate the cLUC-NB and nLUC-PP2C4 constructs, the coding sequences of Sw-5b-NB and PP2C4 were amplified by PCR, and cloned into the *35Spro*: cLUC and *35Spro*: nLUC vectors⁵⁴.

All primers used in this study are listed in Supplementary Table 2, and all constructs were verified by sequencing.

Y2H screening and assays

Y2H screening was performed as reported previously⁵⁵. Briefly, the Sw-5b-NB were cloned into the pGBKT7 vector (Clontech) and transformed into the Y2H-gold yeast strain. Yeast cells containing pGBKT7-Sw-5b-NB were mated with the *N. benthamiana* cDNA prey library, which was constructed on the previously described pGADT7 prey vector⁵⁵ at 30 °C and 50 rpm for 20 h. The fusion cells were incubated

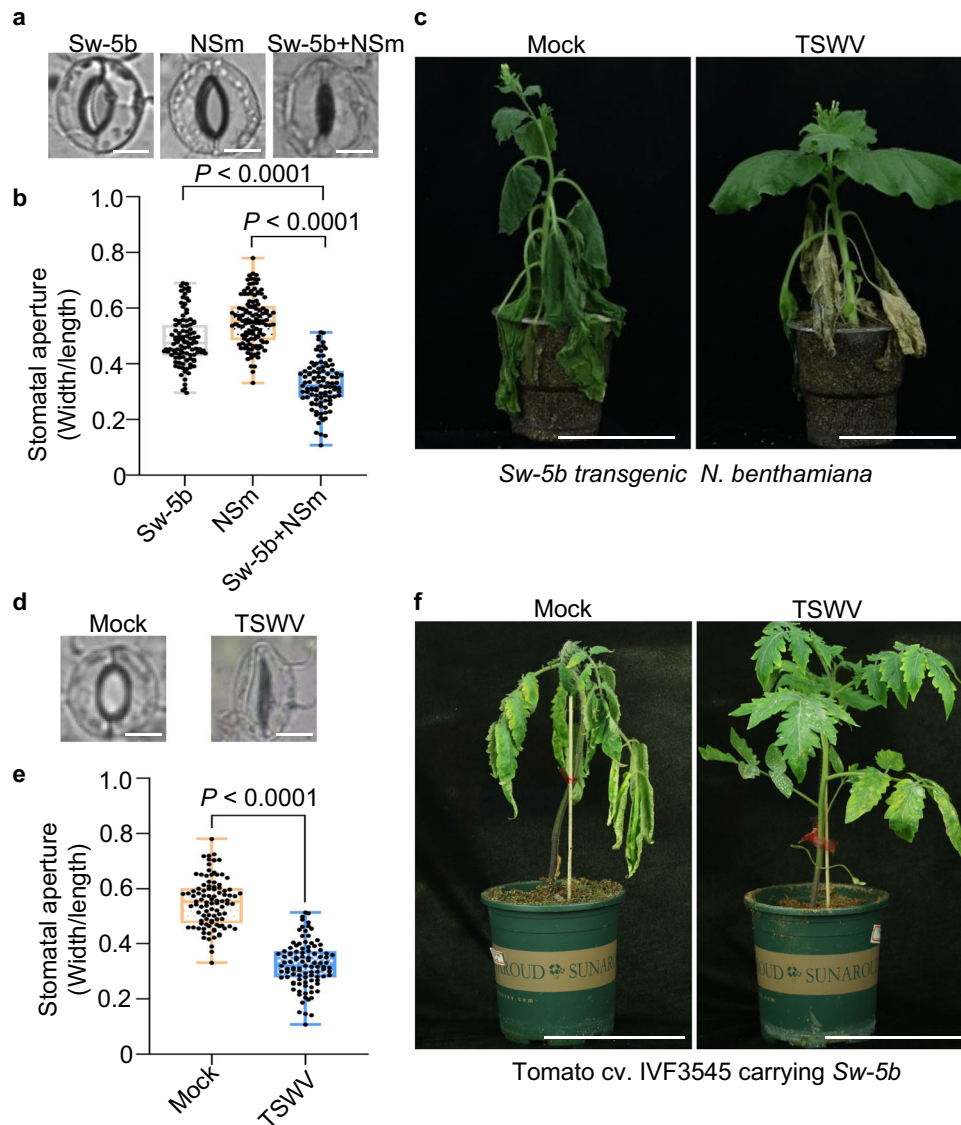


Fig. 5 | Sw-5b NLR induces plant stomatal closure and drought resistance in *N. benthamiana* and tomato plants upon recognition of viral effector NSm. **a** Co-expression of Sw-5b and NSm induces stomatal closure in *N. benthamiana* leaves. Sw-5b, NSm or Sw-5b and NSm were (co)expressed in *N. benthamiana* leaves via agroinfiltration. The stomatal aperture was measured at 24 hpi. Bars = 10 μ m. **b** Statistical analysis results of stomatal aperture in leaves treated with Sw-5b, NSm, or Sw-5b and NSm via agroinfiltration. **c** Sw-5b-transgenic *N. benthamiana* plants inoculated with TSWV-infected leaf sap were assayed for drought resistance through water shortage treatment for 10 days. Plants rub-inoculated with sap from healthy plant leaf tissues were used as mock controls. Bars = 8 cm. Experiments were repeated three times with similar results. **d** Stomatal closure analysis of tomato

leaves (+Sw-5b) inoculated with TSWV or mock control at 4 dpi. Bars = 10 μ m. **e** Statistical analysis results of stomatal aperture in tomato leaves treated with TSWV or mock control, as shown in panel **d**. **f** Tomato plants carrying the Sw-5b resistance gene inoculated with TSWV-infected leaf sap were assayed for drought resistance through water shortage treatment for 10 days. Plants rub-inoculated with sap from healthy plant leaf tissues were used as mock controls. Bars = 12 cm. **b**, **e** Data were shown as the box plots with the interquartile range as the upper and lower confines, minima and maxima as whiskers, and the median as a solid line ($n = 100$, the number of stomata); the exact P value (two-sided Student's t -test) is provided in Source Data. Source data are provided as a Source Data file. All experiments were repeated at least three times with similar results.

at 28 °C on an SD/-TLHA medium plate for 5 days. Positive prey clones grown on SD/-TLHA medium were propagated in Leu-deficient medium to extract the plasmid and co-transformed into Y2H-gold yeast cells together with pGBKT7-Sw-5b-NB to confirm their interactions. The insert of the positive clones that interacted with Sw-5b NB was sequenced and analyzed by BLASTn.

For the Y2H assays, gold yeast strain cells were transformed with various combinations of BD- and AD-derived constructs and were grown at 28 °C for 3 days on the SD/-Trp-Leu medium. The yeast cells were diluted in ddH₂O at ratios of 1:1, 1:10, 1:100, and 1:1000 (v/v) and grown on SD/-Trp-Leu and SD/-Trp-Leu-His-Ade media for 3 days at 28 °C. Yeast transformed with BD-P53 and AD-SV40T was used as a positive control.

SLC assay

Agrobacterium-mediated transient expression in *N. benthamiana* leaves was performed following the method of ref. 39. All constructs used in this study were transformed into *Agrobacterium tumefaciens* strain GV3101, grown to an optical density at 600 nm (OD₆₀₀) of 0.8–1.0, centrifuged at 6000 rpm for 10 min, and then resuspended with an infiltrating buffer (10 mM MES [pH 5.6], 10 mM MgCl₂, and 150 mM acetosyringone) to OD₆₀₀ = 0.2. The cell suspension mixture was infiltrated into the abaxial (lower) side of *N. benthamiana* leaves using a 2-mL needleless syringe.

The SLC assay was performed according to the method of Chen et al. with slight modifications⁵⁴. *Agrobacterium tumefaciens* GV3101 strains carrying different combinations of constructs expressing

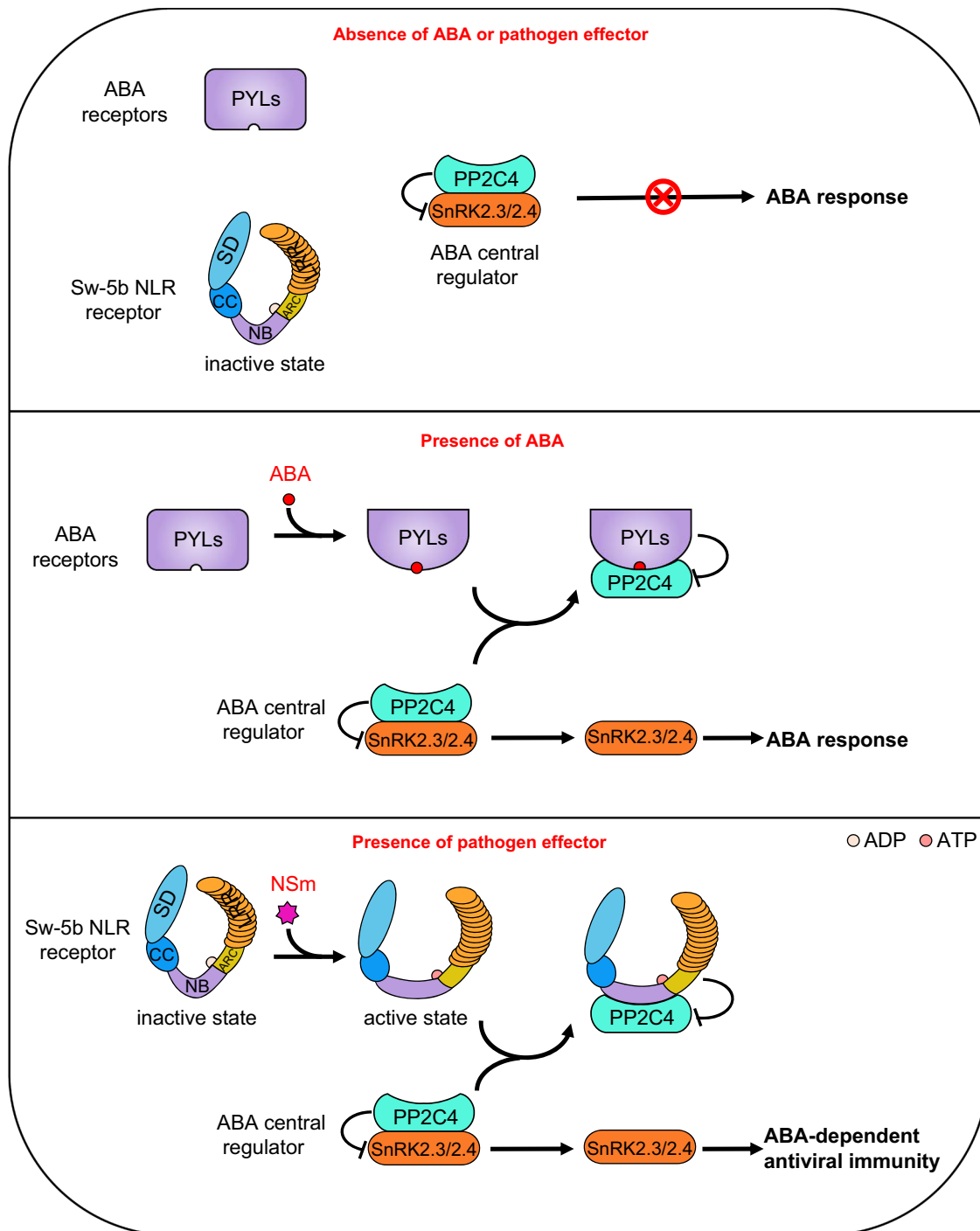


Fig. 6 | A proposed model that the Sw-5b NLR immune receptor mimics the behavior of the ABA receptors and directly modulates the ABA central regulator PP2C-SnRK2 to activate antiviral immunity. At the center of the ABA signaling regulation, PP2C4 interacts with and constitutively inhibits SnRK2.3/2.4. Upon detection of ABA, the ABA receptors PYLs undergo a conformational change that allows them to bind to PP2C4. This binding releases SnRK2 from PP2C inhibition, thereby allowing SnRK2 to activate the downstream ABA signaling pathway (upper). The Sw-5b NLR immune receptor behaves in a similar manner to ABA

receptors to activate ABA signaling. Sw-5b NLR is maintained in an inactive state in the absence of the viral effector NSm. Upon detection of the viral effector NSm, Sw-5b NLR switches from an inactive state to an active state. The conformational changes of Sw-5b allow it to bind to PP2C4 through its NB domain, and this binding interferes with the interaction between PP2C4 and SnRK2.2/2.4, thereby releasing SnRK2 from PP2C-mediated inhibition to activate ABA-dependent antiviral immunity (lower).

cLUC-Sw-5b NB, nLUC-PP2C4, cLUC, or nLUC were infiltrated into *N. benthamiana* leaves. After 36 h of infiltration, the leaves were treated with 150 µg/mL of luciferin potassium salt (Yeasen, Shanghai, China) in the dark for 15 min. Luciferase activity was captured by a low-light cold charge-coupled imaging apparatus (Vilber, Ile-de-France, France).

Antibody preparation

For the detection of NSm and N proteins, a 6×His tag was fused with the proteins, expressed in *E. coli* Rosetta (DE3) cells, and purified using Ni-NTA agarose (Qiagen). The purified NSm or N protein was injected into rabbits to produce polyclonal antibodies.

Co-IP assays

For Co-IP assays, 1 g of agro-infiltrated *N. benthamiana* leaves was harvested and ground in 2 mL of chilled extraction buffer (10% [v/v] glycerol, 25 mM Tris-HCl [pH 7.5], 1 mM EDTA, 150 mM NaCl, 10 mM dithiothreitol, 2% [w/v] polyvinylpyrrolidone, 0.5% [v/v] Triton X-100, and protease inhibitor cocktail) using a mortar and pestle. The mixture was centrifuged at $18,000 \times g$ for 30 min at 4 °C. The supernatant was incubated with 30 μ L of anti-FLAG (Sigma-Aldrich, St. Louis, MO, USA) agarose beads for 2 h at 4 °C. After incubation, the beads were washed four times with IP (50 mM Tris-Cl [pH 8.5], 100 mM NaCl, and 1 mM EDTA) buffer, resuspended in sodium dodecyl-sulfate-polyacrylamide gel electrophoresis (SDS-PAGE) loading buffer (150 mM Tris-HCl, pH = 6.8, 30% glycerol, 6% SDS, 0.3% bromophenol blue, and 300 mM DTT), and boiled at 95 °C for 10 min. The proteins were separated by SDS-PAGE and transferred to polyvinylidene fluoride membranes. The blots were detected using anti-YFP (Sigma-Aldrich, Cat. # SAB4301138, 1:10,000), anti-FLAG (Sigma-Aldrich, Cat. # A8592, 1:10,000), and anti-NSm (made in this study, 1:5,000) followed with Goat Anti-Rabbit IgG-HRP secondary antibody (Sigma-Aldrich, Cat # A0545, 1:10,000). The blots were stained with Ponceau S to estimate protein loading. The uncropped blots are provided in the Source Data file.

qRT-PCR

Total RNA was extracted from *N. benthamiana* and tomato leaves using a FastPure Universal Plant Total RNA Isolation Kit (Vazyme Biotech, Nanjing, China) according to the manufacturer's instructions. The extracted RNA was reverse-transcribed into cDNA by HiScript III RT SuperMix (Vazyme Biotech). We performed qRT-PCR using ChamQ Universal SYBR qPCR Master Mix (Vazyme Biotech) on an ABI Prism 7500 Fast Real-Time PCR system (Life Technologies, Beverly, MA, USA). *NbActin* and *SlActin* were used as internal controls. Primers were designed using Primer Premier 5 software and are listed in Supplementary Table 2.

ABA hormone measurement

Fresh plant material (100 mg) was ground into powder using liquid nitrogen in a mill. The powdered sample was homogenized in 1 mL of extraction buffer (isopropyl alcohol:water:hydrochloric acid, 2:1:0.002) and incubated at 4 °C for 1 h. Dichloromethane (2 mL) was added to the mixture, which was then incubated for 30 min. After centrifugation at $18,000 \times g$ for 15 min at 4 °C, the organic layer of the solution was absorbed and dried through evaporation under a nitrogen gas stream. The dried powder was reconstituted in methanol, and the solution was filtered through a 0.22- μ m filter. The ABA content of samples was analyzed using a Triple Quadrupole Xevo TQ-S System (Waters Corp., Milford, MA, USA) equipped with an ESI ion source and a Waters ACQUITYUPLCBEH C18 column (2.1 mm YUPLCB, 1.71 mm).

Generation of *Nbpp2c4* knockout *N. benthamiana* lines using a CRISPR/Cas9-based technology

Nbpp2c4 knockout mutants were generated using CRISPR/Cas9-based technology following the method of ref. 55. Briefly, leaf disks from 8-week-old *N. benthamiana* plants sterilized with 70% ethanol and 10% sodium hypochlorite solution were incubated in a culture of *A. tumefaciens* carrying BGK01-NbPP2C4 for 15 min at 28 °C. Subsequently, the leaf disks were incubated on a co-cultivation medium for 2 days at 25 °C in the dark. After co-cultivation, the leaf disks were transferred to a shoot regeneration medium and incubated in a growth chamber for 15–20 days until the shoots reached a length of 1–2 cm. The shoots were then separated from the callus and transferred to a rooting medium for 20–30 days. When the roots reached a length of 3–5 cm, the plants were transferred into soil and grown in a greenhouse. Genomic DNA was extracted from regenerated plants, and the targeted sites of *NbPP2C4* were PCR-amplified and sequenced to confirm

that the *NbPP2C4* genes were indeed knocked out. Homozygous T2 lines were used in subsequent experiments.

VIGS

VIGS was performed following the method of ref. 55. A mixture of *Agrobacterium* cells harboring both pTRV1 and pTRV2-NbSnRK2.3/2.4, pTRV2-NbABA2, pTRV2-SIPP2C4, pTRV2-SIABA2, or pTRV2-GUS was co-infiltrated into leaves of 4-week-old *N. benthamiana* or tomato plants. At 3 weeks post-agroinfiltration, the upper leaves of the infiltrated plants were analyzed for gene silencing efficiency. The leaves of plants with high silencing efficiency were used for TSWV inoculation and other experiments.

Seed germination and root elongation assays

The effects of ABA on seed germination and root growth of *NbPP2C4* knockout mutant lines were evaluated following the method of Rubio et al. with slight modifications⁵⁶. For seed germination assays, approximately 80 seeds per experiment were grown on Murashige and Skoog (MS) medium supplemented with or without 2 μ M ABA (Sigma-Aldrich) in a growth chamber under a 16-h light (25 °C; white light, 4000 lumens)/8-h dark (23 °C) photoperiod. After 10 days of incubation, the seedling greening ratio was calculated, and the phenotypes were photographed.

For the root growth inhibition assay, surface-sterilized seeds were sown on MS agar medium supplemented with or without 0.3 μ M ABA. Root elongation was measured and photographed after the plates were grown in a growth chamber for 15 days.

TSWV mechanical inoculation and *Agrobacterium*-mediated inoculation of infectious clones

For TSWV mechanical inoculation, TSWV-infected *N. benthamiana* leaf tissues were harvested and ground in 1 \times phosphate buffer (137 mM NaCl, 2.7 mM KCl, 10 mM Na₂HPO₄, and 2 mM KH₂PO₄, pH 7.4). Leaf sap was rub-inoculated onto the leaves of 4–6-week-old *N. benthamiana* or tomato plants. Plants were either VIGS pretreated, transiently overexpressed with proteins, or treated with ABA. The inoculated plants were grown in a growth chamber under a 16-h light (25 °C)/8-h dark (23 °C) photoperiod.

Agrobacterium-mediated inoculation of infectious clones was conducted as previously described in ref. 42. A mixture of *A. tumefaciens* harboring the TSWV full-length infectious clones of L_{(+)opt}, M_{(-)opt}, and SR_{(+)eGFP} was co-infiltrated into the leaves of 4–6-week-old *N. benthamiana* plants in various assays, as described above.

Y3H assays

For Y3H assays, constructs of AD-PP2C4 and either BD-SnRK2.3-YFP/NB or BD-SnRK2.4-YFP/NB were co-transformed into the Y2H-gold yeast strain and incubated at 28 °C on SD/-Trp-Leu medium for 3 days. Individual colonies were picked and cultured in a liquid medium lacking Trp overnight. The yeast culture was centrifuged at 3000 rpm. The pellet was resuspended in ddH₂O and adjusted to OD₆₀₀ = 1.0. The yeast cells were then diluted at ratios of 1:1 (undiluted), 1:10, 1:100, and 1:1000 (v/v) with ddH₂O and plated on SD/-Trp-Leu and SD/-Trp-Leu-His-Ade-Met solid media at 28 °C for 3 days.

GST pull-down assays

Proteins were expressed in the *E. coli* 'Rosetta' (DE3) strain and purified as previously described³⁹. For the GST pull-down assays, the GST-SnRK2.3/2.4 proteins were mixed with FLAG-PP2C4 and incubated with 30 μ L glutathione-agarose beads for 1.5 h at 4 °C. The beads were washed with pre-cold IP buffer (50 mM Tris-Cl [pH 8.5], 100 mM NaCl, 1 mM EDTA) and then incubated with 1, 5, or 10 μ g YFP-NB, or 10 μ g YFP protein at 4 °C for 1 h. After four washes with IP buffer, protein complexes bound onto the beads were boiled and separated by SDS-PAGE. The proteins were then transferred onto blots and detected with anti-

GST (Sigma-Aldrich, Cat. # SAB1305539, 1:5,000), anti-FLAG (Sigma-Aldrich, Cat. # A8592, 1:10,000), and anti-YFP (Sigma-Aldrich, Cat. # SAB4301138, 1:10,000) antibodies, followed with Goat Anti-Rabbit IgG-HRP secondary antibody (Sigma-Aldrich, Cat # A0545, 1:10,000).

Stomatal aperture and drought resistance assays

Stomatal apertures in epidermal strips peeled from *N. benthamiana* leaves transiently expressing NSm, Sw-5b, and Sw-5b+NSm, or tomato leaves inoculated with TSWV, were photographed and measured using ImageJ software (National Institutes of Health, Bethesda, MD, USA). Drought resistance assays were performed using 6-week-old *Sw-5b* transgenic *N. benthamiana* plants or 8-week-old tomato plants harboring the *Sw-5b* resistance gene. The *N. benthamiana* or tomato plants were rub-inoculated with sap from TSWV-infected *N. benthamiana* leaf tissues, whereas plants rub-inoculated with sap from healthy *N. benthamiana* leaf tissues were used as controls. The plants were then deprived of water for 10 days under the same growing conditions and subsequently photographed.

Quantification and statistical analyses

All statistical analyses were performed by two-sided Student's *t*-test using GraphPad Prism 9 (GraphPad Software, Boston, MA, USA). Data for quantification analyses are presented as means \pm s.d. or as box plots with the interquartile range as the upper and lower confines, minima and maxima as whiskers, and the median as a solid line. Quantification analyses of protein abundance were conducted using ImageJ. Significance was determined at $P < 0.05$.

Reporting summary

Further information on research design is available in the Nature Portfolio Reporting Summary linked to this article.

Data availability

All data were available within this article and its supplementary files. All constructs and transgenic plants are available upon request. The PP2C4 and SnRK2 gene sequences are available from the Sol Genomics Network (<https://www.sgn.cornell.edu/>) using the accession numbers provided in this article. Source data are provided with this paper.

References

- Jones, J. D. G. & Dangl, J. L. The plant immune system. *Nature* **444**, 323–329 (2006).
- Jones, J. D., Vance, R. E. & Dangl, J. L. Intracellular innate immune surveillance devices in plants and animals. *Science* **354**, 6395–6403 (2016).
- Ngou, B. P. M., Ding, P. & Jones, J. D. G. Thirty years of resistance: zig-zag through the plant immune system. *Plant Cell* **34**, 1447–1478 (2022).
- Couto, D. & Zipfel, C. Regulation of pattern recognition receptor signaling in plants. *Nat. Rev. Immunol.* **16**, 537–552 (2016).
- Zhou, J. M. & Zhang, Y. Plant immunity: danger perception and signaling. *Cell* **181**, 978–989 (2020).
- Peng, Y., van Werssch, R. & Zhang, Y. Convergent and divergent signaling in PAMP-Triggered Immunity and effector-triggered immunity. *Mol. Plant Microbe Interact.* **31**, 403–409 (2018).
- Tsuda, K. & Katagiri, F. Comparing signaling mechanisms engaged in pattern-triggered and effector-triggered immunity. *Curr. Opin. Plant Biol.* **13**, 459–465 (2010).
- Cui, H., Tsuda, K. & Parker, J. E. Effector-triggered immunity: from pathogen perception to robust defense. *Annu. Rev. Plant Biol.* **66**, 487–511 (2015).
- Yuan, M. et al. Pattern-recognition receptors are required for NLR-mediated plant immunity. *Nature* **592**, 105–109 (2021).
- Tian, H. N. et al. Activation of TIR signalling boosts pattern-triggered immunity. *Nature* **598**, 500–503 (2021).
- Pruitt, R. N. et al. The EDS1-PAD4-ADR1 node mediates *Arabidopsis* pattern-triggered immunity. *Nature* **598**, 495–499 (2021).
- Ngou, B. P. M., Ahn, H. K., Ding, P. T. & Jones, J. D. G. Mutual potentiation of plant immunity by cell-surface and intracellular receptors. *Nature* **592**, 110–115 (2021).
- Pieterse, C. M. J., Van der Does, D., Zamioudis, C., Leon-Reyes, A. & Van Wees, S. C. M. Hormonal modulation of plant immunity. *Annu. Rev. Cell Dev. Biol.* **28**, 489–521 (2012).
- Aerts, N., Pereira Mendes, M. & Van Wees, S. C. M. Multiple levels of crosstalk in hormone networks regulating plant defense. *Plant J.* **105**, 489–504 (2021).
- Mauch-Mani, B. & Mauch, F. The role of abscisic acid in plant-pathogen interactions. *Curr. Opin. Plant Biol.* **8**, 409–414 (2005).
- Fan, J., Hill, L., Crooks, C., Doerner, P. & Lamb, C. Abscisic acid has a key role in modulating diverse plant-pathogen interactions. *Plant Physiol.* **150**, 1750–1761 (2009).
- Alazem, M., Lin, K. Y. & Lin, N. S. The abscisic acid pathway has multifaceted effects on the accumulation of Bamboo mosaic virus. *Mol. Plant Microbe Interact.* **27**, 177–189 (2014).
- Iriti, M. & Faoro, F. Abscisic acid is involved in chitosan-induced resistance to tobacco necrosis virus (TNV). *Plant Physiol. Biochem.* **46**, 1106–1111 (2008).
- He, L. et al. Comparative proteomic analysis of *Nicotiana benthamiana* plants under Chinese wheat mosaic virus infection. *BMC Plant Biol.* **21**, 51 (2021).
- Seo, J. K., Kwon, S. J., Cho, W. K., Choi, H. S. & Kim, K. H. Type 2 C protein phosphatase is a key regulator of antiviral extreme resistance limiting virus spread. *Sci. Rep.* **4**, 5905 (2014).
- Raghavendra, A. S., Gonugunta, V. K., Christmann, A. & Grill, E. ABA perception and signaling. *Trends Plant Sci.* **15**, 395–401 (2010).
- Zhu, J. K. Abiotic stress signaling and responses in plants. *Cell* **167**, 313–324 (2016).
- Hirayama, T. & Shinozaki, K. Perception and transduction of abscisic acid signals: keys to the function of the versatile plant hormone ABA. *Trends Plant Sci.* **12**, 343–351 (2007).
- Santiago, J. et al. The abscisic acid receptor PYR1 in complex with abscisic acid. *Nature* **462**, 665–668 (2009).
- Melcher, K. et al. A gate-latch-lock mechanism for hormone signaling by abscisic acid receptors. *Nature* **462**, 602–608 (2009).
- Park, S. Y. et al. Abscisic acid inhibits type 2 C protein phosphatases via the PYR/PYL family of START proteins. *Science* **324**, 1068–1071 (2009).
- Schweighofer, A., Hirt, H. & Meskiene, I. Plant PP2C phosphatases: emerging functions in stress signaling. *Trends Plant Sci.* **9**, 236–243 (2004).
- Leung, J., Merlot, S. & Giraudat, J. The *Arabidopsis* ABSCISIC ACID-INSENSITIVE2 (ABI2) and ABI1 genes encode homologous protein phosphatases 2 C involved in abscisic acid signal transduction. *Plant Cell* **9**, 759–771 (1997).
- Fujii, H. et al. In vitro reconstitution of an abscisic acid signalling pathway. *Nature* **462**, 660–664 (2009).
- Soon, F. F. et al. Molecular mimicry regulates ABA signaling by SnRK2 kinases and PP2C phosphatases. *Science* **335**, 85–88 (2012).
- Fujii, H., Verslues, P. E. & Zhu, J. K. Identification of two protein kinases required for abscisic acid regulation of seed germination, root growth, and gene expression in *Arabidopsis*. *Plant Cell* **19**, 485–494 (2007).
- Oliver, J. E. & Whitfield, A. E. The genus Tospovirus: emerging Bunyaviruses that threaten food security. *Annu. Rev. Virol.* **3**, 101–124 (2016).
- Scholthof, K. B. et al. Top 10 plant viruses in molecular plant pathology. *Mol. Plant Pathol.* **12**, 938–954 (2011).
- Zhu, M., van Grinsven, I. L., Kormelink, R. & Tao, X. Paving the way to tospovirus infection: multilined interplays with plant innate immunity. *Annu. Rev. Phytopathol.* **57**, 41–62 (2019).

35. Brommonschenkel, S. H., Frary, A., Frary, A. & Tanksley, S. D. The broad-spectrum tospovirus resistance gene Sw-5 of tomato is a homolog of the root-knot nematode resistance gene Mi. *Mol. Plant Microbe Interact.* **13**, 1130–1138 (2000).
36. Spassova, M. I. et al. The tomato gene Sw5 is a member of the coiled coil, nucleotide binding, leucine-rich repeat class of plant resistance genes and confers resistance to TSWV in tobacco. *Mol. Breed.* **7**, 151–161 (2001).
37. Zhu, M. et al. The intracellular immune receptor Sw-5b confers broad-spectrum resistance to tospoviruses through recognition of a conserved 21-amino acid viral effector epitope. *Plant Cell* **29**, 2214–2232 (2017).
38. Feng, Z. et al. Nucleocapsid of Tomato spotted wilt tospovirus forms mobile particles that traffic on an actin/endoplasmic reticulum network driven by myosin XI-K. *N. Phytol.* **200**, 1212–1224 (2013).
39. Li, J. et al. A plant immune receptor adopts a two-step recognition mechanism to enhance viral effector perception. *Mol. Plant* **12**, 248–262 (2019).
40. Zhao, X. et al. The Sw-5b NLR nucleotide-binding domain plays a role in oligomerization, and its self-association is important for activation of cell death signaling. *J. Exp. Bot.* **72**, 6581–6595 (2021).
41. Shirasu, K. The HSP90-SGT1 chaperone complex for NLR immune sensors. *Annu. Rev. Plant Biol.* **60**, 139–164 (2009).
42. Chen, X. et al. A multilayered regulatory mechanism for the auto-inhibition and activation of a plant CC-NB-LRR resistance protein with an extra N-terminal domain. *N. Phytol.* **212**, 161–175 (2016).
43. Chen, H. et al. Cytoplasmic and nuclear Sw-5b NLR act both independently and synergistically to confer full host defense against tospovirus infection. *N. Phytol.* **231**, 2262–2281 (2021).
44. Feng, M. F. et al. Rescue of tomato spotted wilt virus entirely from complementary DNA clones. *Proc. Natl Acad. Sci. USA* **117**, 1181–1190 (2020).
45. Feng, Z. et al. The ER-membrane transport system is critical for intercellular trafficking of the NSm movement protein and tomato spotted wilt tospovirus. *PLoS Pathog.* **12**, e1005443 (2016).
46. Nakashima, K. et al. Three *Arabidopsis* SnRK2 protein kinases, SRK2D/SnRK2.2, SRK2E/SnRK2.6/OST1 and SRK2I/SnRK2.3, involved in ABA signaling are essential for the control of seed development and dormancy. *Plant Cell Physiol.* **50**, 1345–1363 (2009).
47. Ma, Y. et al. Regulators of PP2C phosphatase activity function as abscisic acid sensors. *Science* **324**, 1064–1068 (2009).
48. Alazem, M. & Lin, N. S. Antiviral roles of abscisic acid in plants. *Front. Plant Sci.* **8**, 1760–1770 (2017).
49. Merlot, S., Gosti, F., Guerrier, D., Vavasseur, A. & Giraudat, J. The ABI1 and ABI2 protein phosphatases 2C act in a negative feedback regulatory loop of the abscisic acid signaling pathway. *Plant J.* **25**, 295–303 (2001).
50. Wang, J. Z. et al. Reconstitution and structure of a plant NLR resistosome conferring immunity. *Science* **364**, 5868–5870 (2019).
51. Tian, D., Traw, M. B., Chen, J. Q., Kreitman, M. & Bergelson, J. Fitness costs of R-gene-mediated resistance in *Arabidopsis thaliana*. *Nature* **423**, 74–77 (2003).
52. Chen, J. et al. NLR surveillance of pathogen interference with hormone receptors induces immunity. *Nature* **613**, 145–152 (2023).
53. Fu, S. et al. An evolutionarily conserved C4HC3-type E3 ligase regulates plant broad-spectrum resistance against pathogens. *Plant Cell* **34**, 1822–1843 (2022).
54. Chen, H. et al. Firefly luciferase complementation imaging assay for protein–protein interactions in plants. *Plant Physiol.* **146**, 368–376 (2008).
55. Wu, Q. et al. NLRs derepress MED10b- and MED7-mediated repression of jasmonate-dependent transcription to activate immunity. *Proc. Natl Acad. Sci. USA* **120**, e2302226120 (2023).
56. Rubio, S. et al. Triple loss of function of protein phosphatases type 2C leads to partial constitutive response to endogenous abscisic acid. *Plant Physiol.* **150**, 1345–1355 (2009).

Acknowledgements

This work is supported by the National Natural Science Foundation of China (Grant Nos. 31925032, 32220103008, and 31972241), the National Key Research and Development Program of China (Grant No. 2022YFF1001500), the Funds from the Independent Innovation of Agricultural Science and Technology of Jiangsu Province [Grant No. CX (22) 2039], the Jiangsu Key Technology R & D Program and International Science and Technology Cooperation Project (Grant No. BZ2023030), the “111” project, the Key Science and Technology Program of Hainan Province (Grant No. ZDKJ2021007), the Guidance Foundation, the Sanya Institute of Nanjing Agricultural University (Grant No. NAUSY-MS19), and Yunnan Seed Laboratory (Grant No. 202205AR070001) to X.T., and the Postgraduate Research & Practice Innovation Program of Jiangsu Province (Grant No. KYCX21_0620) to S.H.

Author contributions

S.H. and X.T. conceived and designed the experiments; J.L., H.H., M.Z., Y.J., Z.Z., and M.F. provided input. S.H., C.W., Z.D., Y.Z., J.D., and T.W. performed the experiments. S.H. and X.T. wrote the paper.

Competing interests

The authors declare no competing interests.

Additional information

Supplementary information The online version contains supplementary material available at <https://doi.org/10.1038/s41467-024-47364-8>.

Correspondence and requests for materials should be addressed to Xiaorong Tao.

Peer review information *Nature Communications* thanks the anonymous reviewers for their contribution to the peer review of this work. A peer review file is available.

Reprints and permissions information is available at <http://www.nature.com/reprints>

Publisher’s note Springer Nature remains neutral with regard to jurisdictional claims in published maps and institutional affiliations.

Open Access This article is licensed under a Creative Commons Attribution 4.0 International License, which permits use, sharing, adaptation, distribution and reproduction in any medium or format, as long as you give appropriate credit to the original author(s) and the source, provide a link to the Creative Commons licence, and indicate if changes were made. The images or other third party material in this article are included in the article’s Creative Commons licence, unless indicated otherwise in a credit line to the material. If material is not included in the article’s Creative Commons licence and your intended use is not permitted by statutory regulation or exceeds the permitted use, you will need to obtain permission directly from the copyright holder. To view a copy of this licence, visit <http://creativecommons.org/licenses/by/4.0/>.

© The Author(s) 2024